Interface focus

J. R. Soc. Interface (2010) **7**, S451–S460
doi:10.1098/rsif.2010.0092.focus
Published online 2 June 2010

Controlling the thickness of hollow polymeric microspheres prepared by electrohydrodynamic atomization

Ming-Wei Chang, Eleanor Stride* and Mohan Edirisinghe

Department of Mechanical Engineering, University College London, Torrington Place, London WC1E 7JE, UK

In this study, the ability to control the shell thickness of hollow polymeric microspheres prepared using electrohydrodynamic processing at ambient temperature was investigated. Polymethylsilsesquioxane (PMSQ) was used as a model material for the microsphere shell encapsulating a core of liquid perfluorohexane (PFH). The microspheres were characterized by Fourier transform infrared spectroscopy and optical and electron microscopy, and the effects of the processing parameters (flow-rate ratio, polymer concentration and applied voltage) on the mean microsphere diameter (D) and shell thickness (t) were determined. It was found that the mean diameters of the hollow microspheres could be controlled in the range from 310 to 1000 nm while the corresponding mean shell thickness varied from 40 to 95 nm. The results indicate that the ratio $D:t$ varied with polymer concentration, with the largest value of approximately 10 achieved with a solution containing 18 wt% of the polymer, while the smallest value (6.6) was obtained at 36 wt%. For polymer concentrations above 63 wt%, hollow microspheres could not be generated, but instead PMSQ fibres encapsulating PFH liquid were obtained.

Keywords: hollow spheres; electrohydrodynamic atomization; perfluorocarbon

1. INTRODUCTION

Spheres with hollow interiors play an important role in microencapsulation and have been used in medical, biological, pharmaceutical and industrial applications (Hu *et al.* 2007; Bai *et al.* 2009; Xiao *et al.* 2009; Yan *et al.* 2009; Zhang *et al.* 2009). Both organic and inorganic materials have been investigated to manufacture new and smart hollow microspheres and offer advantages such as low effective density, large internal 'payload' space and high specific surface area (Lou *et al.* 2008; Shiomi *et al.* 2009; Zimmermann *et al.* 2009). Hollow polymer spheres, in particular those with single core/shell structures, have stimulated great interest in encapsulating sensitive materials, e.g. drugs, markers, DNA and field-responsive agents (Dowding *et al.* 2004; Xu & Asher 2004). In addition, the investigation of hollow polymer microspheres with different and controllable shell thickness has become increasingly important as a result of their superior mechanical properties and release behaviour in medical and pharmaceutical applications (Li, G. *et al.* 2007; Liu, G. *et al.* 2007; Gao *et al.* 2009).

Several techniques, such as hard template (Wu *et al.* 2000), polymeric micelles (Chen & Jiang 2005), dynamic swelling (Okubo *et al.* 2000) and emulsification (Utada *et al.* 2005; Zoldesi & Imhof 2005), have been explored extensively to generate a variety of such microspheres. Various materials and liquids are used as templates for hollow spheres to provide effective control over cavity size and a highly selective etching ratio (Caruso *et al.* 1998; Lynch *et al.* 2005). The hollow structure may be obtained after removal of the template core by selective dissolution in an appropriate solvent or by calcination at high temperature (Wang & Caruso 2002). The ratio of wall thickness to diameter can be varied by different processes. However, the formation of a shell with a predetermined shell thickness and properties requires a time-consuming synthetic process, normally requiring surfactants or amphiphilic polymers to increase kinetic stability (Kim & Yoon 2004; Song *et al.* 2006; Daiguji *et al.* 2007). In addition, the template-removal step not only increases the processing time and cost, it may also result in damage to the shells (Liu, Q. *et al.* 2007).

Electrohydrodynamic atomization (EHDA) is an attractive method for preparing particulate polymeric carriers with sizes ranging from several tens of nanometres to approximately 100 μm for the pharmaceutical, cosmetic and food industries, as well as several other technological fields (Pareta & Edirisinghe 2006; Xie *et al.* 2006; Farook *et al.* 2009; Valo *et al.* 2009). This strategy has distinct differences and advantages in comparison with conventional approaches. There is no template production, which not only

*Author for correspondence (e_stride@meng.ucl.ac.uk).

One contribution to a Theme Supplement 'Scaling the heights—challenges in medical materials: an issue in honour of William Bonfield, Part I. Particles and drug delivery'.

Received 17 February 2010
Accepted 12 May 2010

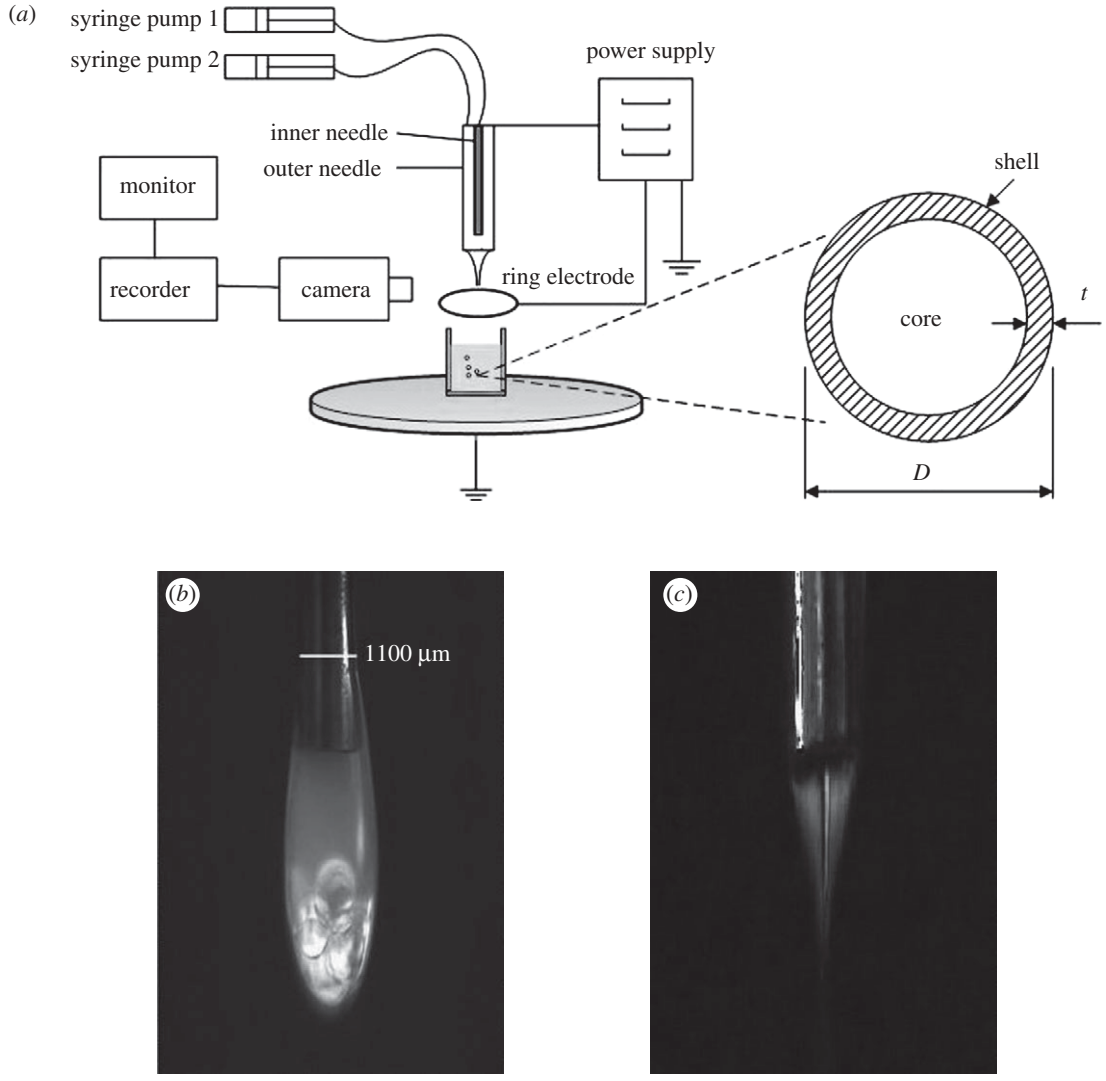

Figure 1. (*a*) The experimental set-up; (*b*) dripping and (*c*) stable jetting behaviour of PMSQ/PFH.

makes the process of hollow polymer microsphere generation more efficient, but also avoids the need for subsequent template removal by calcination or chemical solutions. Similarly, there is no need for a separate shell-forming step, which further avoids the use of surfactants or other additives.

However, despite its versatility and growing popularity, the question as to whether EHDA can be used to generate hollow microspheres with predetermined characteristics remains unanswered. Characteristics such as particle diameter, shell thickness, diffusivity and uniformity are very important in many cases for both fundamental research and practical applications. If these characteristics can be controlled, then it is possible to tailor the capsule shell to control the exchange of the encapsulated substance(s) with an external medium (Shchukin *et al.* 2003; Wang *et al.* 2007), to control the particle's mechanical properties and its transportation behaviour (Qiu *et al.* 2001; Dong *et al.* 2005; Rachik *et al.* 2006).

The objectives of this study were to demonstrate the fabrication of hollow polymeric microspheres by EHDA and to determine the effect of individual processing parameters upon the shell thickness (t) and microsphere diameter (D) (figure 1*a*). Specifically, the effects of changing the flow-rate ratio, polymer concentration and applied voltage upon the particle morphology and ratio $D\colon t(\alpha)$ were investigated in detail.

2. EXPERIMENTAL SECTION

2.1. Materials

Polymethylsilsesquioxane (PMSQ) was used as a model shell material while perfluorohexane (PFH) was used to form the microsphere cores. Both materials are chemically stable and biocompatible. In addition, PMSQ can be pyrolysed to directly make ceramic (SiO_xC_y) hollow spheres (Nangrejo *et al.* 2008). PFH was obtained from F2 Chemicals Ltd (Lea, UK) and was used without further treatment. PMSQ was obtained from Wacker Chemie AG, GmbH (Burghausen, Germany). Ethanol was obtained from BDH Laboratory Supplies (London, UK) and used to prepare solutions of PMSQ of different concentrations by dissolving with magnetic stirring in a conical flask for 1800 s at 22°C to ensure full miscibility of the polymer. Distilled water was used for all experiments.

Table 1. Measured physical properties of the liquids used in experimental work.

material	density (kg m^{-3})	viscosity (mPa s)	surface tension (mN m^{-1})	electrical conductivity (S m^{-1})
perfluorohexane	1710	1.1	12	$<1 \times 10^{-11}$
PMSQ 18 wt%	805	1.8	23	9×10^{-5}
PMSQ 27 wt%	834	2.9	23	8×10^{-5}
PMSQ 36 wt%	861	5.2	23	6×10^{-5}
PMSQ 63 wt%	993	53	26	1×10^{-5}

2.2. Characterization of solutions

The physical properties of the liquids being processed play an important role in EHDA since, together with the processing conditions (i.e. needle size; Li, X. *et al.* 2007), working distance (Berkland *et al.* 2004), flow rate (Lastowa & Balachandran 2006) and applied voltage (de la Mora & Loscertales 1994), they determine the electrospraying mode and hence also the size (Xie *et al.* 2006), shape (Berkland *et al.* 2004) and morphology (Munir *et al.* 2009) of relics formed. The viscosity, density, surface tension and electrical conductivity of the polymer solutions were characterized as follows. Viscosity was determined using a U-tube viscometer and a Viscoeasy rotational viscometer. Density was measured using a standard 25 ml density bottle. Surface tension was measured using a Kruss tensiometer. Electrical conductivity was determined using an HI-8733 conductivity probe. The properties of PFH were provided by the standard data sheet from F2 Chemicals Ltd (2010). Ethanol was used to calibrate the various instruments mentioned above and all experiments were performed at the ambient pressure and temperature (22°C).

2.3. Fabrication of hollow microspheres

A schematic of the experimental set-up used for preparing the microspheres is shown in figure 1*a* and consisted of a pair of concentric needles, with the inner needle raised by 2 mm above the exit of the outer needle. The outer needle had outer and inner diameters of 1100 and 685 μm, respectively. The inner needle had an outer diameter of 300 μm and an inner diameter of 150 μm. The inner stainless steel needle was supplied with PFH, while the PMSQ solution was introduced through the outer needle. The flow rates of the two liquids were controlled by high-precision programmable syringe pumps (Harvard PHD 4400, Apparatus, Edenbridge, UK). Syringes with volume capacities of 10 and 5 ml were separately connected to the inner and outer needles using silicone tubing. A high-voltage generator (Glassman Europe Ltd, Bramley, UK) was connected to provide the electric field between the needles and a ring-shaped ground electrode (external and internal diameter of 20 and 15 mm, respectively). The distance from the exit of the outer needle to the ground electrode (the working distance) was fixed at 12 mm in all the experiments.

To visualize the flow of the liquids under the influence of the electric field, a video camera (Leica S6D JVC-colour) was focused upon the needle outlet and the video signals transmitted to a data recorder and monitor. The microspheres were collected in a glass vial containing distilled water, positioned just below the ring-shaped electrode (figure 1*a*). A 100 × 150 mm filter (grade 105) was used to remove solidified lumps of polymer collected with the microspheres, and subsequently the microspheres were transferred to a new glass vial.

2.4. Characterization of microspheres

The size and surface morphology of the fabricated particles were studied by optical microscopy (Nikon Eclipse ME-600, Nikon Co., Tokyo, Japan) and scanning electron microscopy (SEM; JEOL JSM-6301F field emission scanning electron microscope). One millilitre samples of the microspheres were collected and put on glass slides. After drying for 48 h in a desiccator, the samples were then vacuum-coated with a thin layer of gold for 90 s to obtain scanning electron microscope images. These particles were examined using SEM at 5 kV. To calculate the size of the capsules, 200 microspheres were analysed from the SEM images.

The shell thickness was measured as follows. The dried microspheres were sectioned using a scalpel blade (no. 21, VWR International Ltd, London, UK) to enable examination of the cross sections of individual microspheres. SEM was used to estimate the shell thickness of the microspheres. The shell thickness was measured at four points per microsphere using 50 particles randomly selected from a batch of 200 microspheres and the mean shell thickness was calculated from these four values. All measurements on the micrographs were carried out using the standard IMAGE-PROPLUS software (Media Cybernetics, L.P. Del Mar, CA, USA).

Fourier transform infrared (FT-IR) spectra were obtained using a Perkin Elmer System 2000 FT-IR spectrometer (PerkinElmer Life and Analytical Sciences, Inc., Wellesley, MA, USA) using the standard KBr pellet technique. All spectra were obtained after KBr background subtraction by averaging 30 scans.

3. RESULTS AND DISCUSSION

3.1. Fabrication method

The measured properties of the materials used in this study are shown in table 1. The two immiscible liquids, PFH and PMSQ solutions, were injected with different flow rates and under different applied voltages to

determine the effect upon microsphere formation. However, to obtain a stable jet in two-phase (co-axial) electrospraying, the characteristics of the 'driving' liquid need to be carefully selected (Loscertales *et al.* 2002), since it is this liquid that accommodates the electrical force and thereby plays the dominant role in the formation of the jet and hence the size and coating thickness of the capsules formed.

In this study, the outer PMSQ solution acted as the driving liquid because of its lower electrical relaxation time (López-Herrera *et al.* 2003) and higher viscosity compared with PFH. The stable jet was not observed in the absence of the PMSQ solution, indicating that the inner liquid (PFH) cannot produce a stable jet because of its low electrical conductivity. Figure 1*b*,*c* shows the electrospraying behaviour of both the PMSQ solution and PFH at different applied voltages. The gravity-driven dripping mode of PMSQ/PFH was observed at zero voltage, while the flow rates of syringe 1 (PFH solution) and syringe 2 (36 wt% PMSQ solution) were fixed at 150 and 300 μl min^{-1}, respectively (figure 1*b*). In this experiment, the dripping mode can be approximately divided into two parts (upper and lower), in which the lower part consists of the PFH droplets surrounded by a thin layer of PMSQ because of the higher density of the inner liquid.

With increasing electric field strength, the dripping mode changes to stable jetting, which was reached at 4.2 kV (figure 1*c*). Jet stability is discussed further in a related paper (Chang *et al.* 2010). Normally, in this mode, the cone volume is largely occupied by the inner liquid, with the outer liquid flowing in a very thin film on the outside of the cone (Loscertales *et al.* 2002). In figure 1*c*, however, it can be seen that there is a liquid interface inside the cone and the inner liquid does not fill the cone volume. This observation can be ascribed to the high density, low electrical conductivity and low miscibility of the PFH liquid and the high polymer concentration. Once the cone-jet is formed, concentric droplets can be generated as the jet breaks up. These droplets are initially highly charged, but lose their charge during collection owing to the presence of the grounded electrode (figure 1*a*).

3.2. Effect of flow rate

The liquid flow rates are often the key controlling parameters during the preparation of structures by EHDA. To determine the influence of the driving liquid, the flow rate of syringe 2 (PMSQ solution 18 wt%) was varied between 200 and 650 μl min^{-1} while the flow rate of syringe 1 (PFH solution) was fixed at 150 μl min^{-1}. Figure 2 shows the effect of increasing the PMSQ solution flow rate on the particle mean diameter (D), which increased from 420 nm at 250 μl min^{-1} to 1000 nm at 650 μl min^{-1}. However, at a flow rate of 200 μl min^{-1}, irregular microspheres with a porous surface were generated instead of spherical microspheres (figure 3*a*). This can be attributed to the outer liquid (PMSQ solution) being unable to provide sufficient driving force (see §3.1) to encapsulate

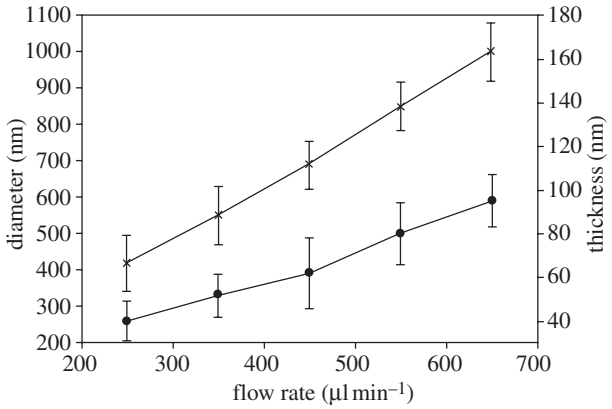

Figure 2. Diameter and shell thickness of microspheres versus varying flow rate of PMSQ and with PFH flow rate of 150 μl min^{-1} (error bars show standard deviation). Line with crosses, D; line with filled circles, t.

the PFH liquid. This kind of hollow microsphere with a porous surface has in fact previously been reported and classified as a new particle on account of the higher effective diffusivity and available surface area compared with microspheres of the same size (Im *et al.* 2005).

Figure 3*a*–*f* shows SEM images of the hollow PMSQ microspheres fabricated at flow rates of PMSQ at 200, 250, 350, 450, 550 and 650 μl min^{-1}, respectively. As above, for liquid flow rates less than 200 μl min^{-1}, microspheres of irregular morphology with a porous surface were generated (figure 3*a*). When the flow rate was fixed greater than 250 μl min^{-1}, the microspheres were spherical with smooth surfaces and a narrow size distribution. However, some of these microspheres were also seen to be interconnected. This is thought to have occurred as a result of liquid residue (water and ethanol) remaining between the PMSQ microspheres when they were transferred to the desiccator for drying. The ethanol subsequently acted as a solvent on very small quantities of the PMSQ shell surface, creating a connection between some of the microspheres. Repeating the 'washing' of the microspheres could eliminate this effect.

The mean shell thickness (t) was also influenced by increasing PMSQ flow rate and similarly increased with increasing flow rate (figure 2). Typical cross sections are presented on the upper right-hand side of figure 3*b*–*f*. It should be noted that the sectioned microspheres were obtained by a destructive method and the non-spherical appearance of some of the particles is due to the applied cutting force. Figure 3*b*–*f* indicates that hollow microspheres with a single cavity were successfully formed and that the shell thickness varied from 40 nm for a mean diameter of 420 nm to 95 nm for a mean diameter of 1000 nm. Furthermore, the D/t ratio (α) showed a slight increase from 10.5 at 250 μl min^{-1} to 10.7 at 650 μl min^{-1}. Figure 4 shows a microsphere with its shell cracked open, and this is further evidence to indicate that the microspheres were not solid capsules but consist of a single internal cavity, which was previously occupied by PFH. If the spheres had been solid with a sponge-like internal

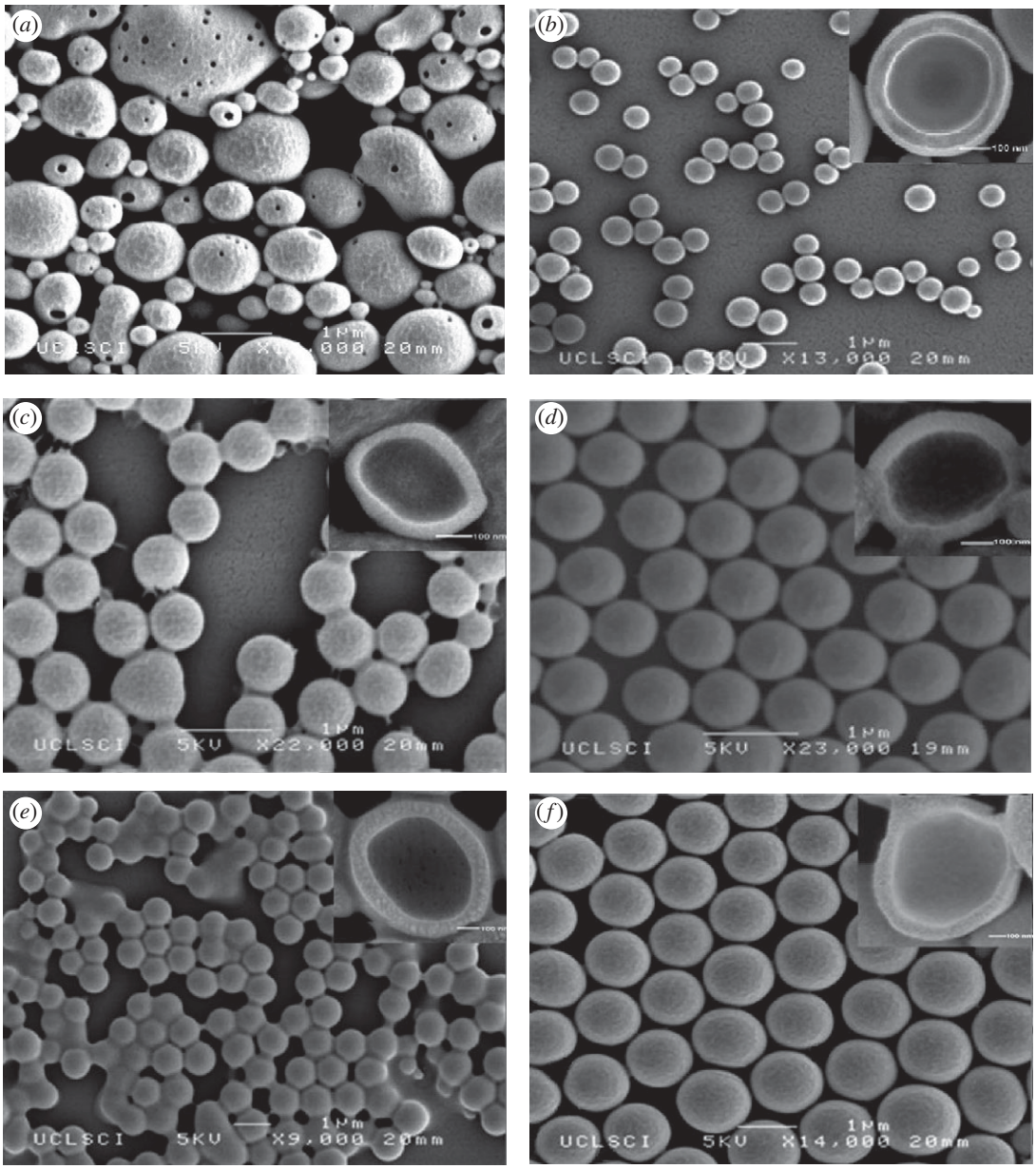

Figure 3. Effect of PMSQ flow rate on the geometry of the hollow microspheres: (*a*) 200; (*b*) 250; (*c*) 350; (*d*) 450; (*e*) 550; and (*f*) 650 μl min^{-1}.

structure, then this would have indicated that the PFH liquid had not been successfully encapsulated.

3.3. Influence of polymer concentration

The effect of PMSQ concentration on the preparation of hollow microspheres was studied for 18, 27, 36 and 63 wt% PMSQ in ethanol. With increasing PMSQ concentration, the viscosity of the solutions increases owing to increased polymer chain entanglement, while electrical conductivity decreases because of the insulating characteristics of PMSQ (table 1). Both parameters would be expected to affect the morphology of the microspheres. The microspheres generated were spherical except at 63 wt% PMSQ. However, increasing the polymer concentration resulted in an increase in the mean microsphere diameter (D) from 460 nm at 18 wt% PMSQ to 630 nm at 36 wt% (figure 5). The increase in particle size may be attributed to the higher surface tension, density and viscosity and the lower electrical conductivity of the higher concentration solutions. The mean shell thickness of the microspheres varied from 45 nm at 18 wt% PMSQ to 95 nm at 36 wt% (figure 5). In addition, the ratio α showed a decrease from 10.2 at 18 wt% to 6.6 at 36 wt%. These effects may similarly be attributed to the higher viscosity and higher surface tension (Hartman *et al.* 1999).

As the polymer concentration was increased to 63 wt%, a transition from electrohydrodynamic spraying to electrospinning was observed. Also, the polymer began to solidify and it became difficult to obtain hollow microspheres by adjusting the applied voltage. Instead, composite fibres were formed as shown in the optical and scanning micrographs in figure 6. Figure 6*a* shows an SEM image of an electrospun fibre

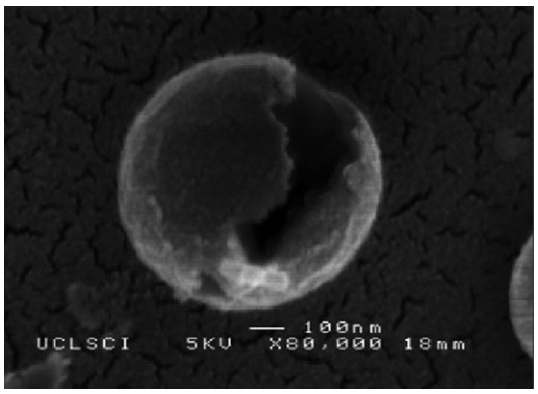

Figure 4. Scanning electron micrograph of a fractured hollow microsphere.

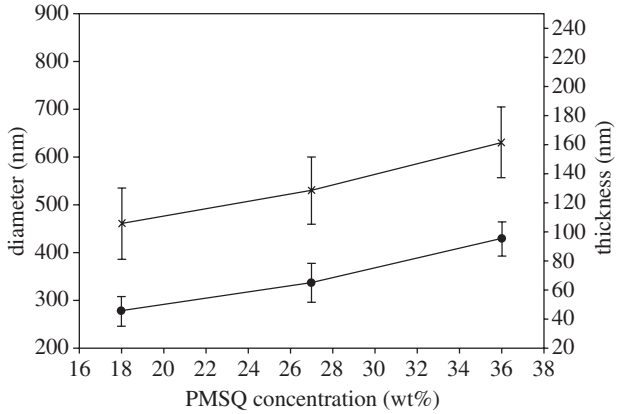

Figure 5. Size and shell thickness of microspheres versus PMSQ concentration with inner flow rates of 150 μl min^{-1} and outer flow rate of 300 μl min^{-1} (error bars show standard deviation). Line with crosses, *D*; line with filled circles, *t*.

prepared at 9.7 kV, whose surface shows both wrinkled and smooth features that are thought to be due to solvent evaporation during collection (Loscertales *et al.* 2002; Berkland *et al.* 2004). Figure 6*b* shows an optical image of the same fibre and provides more detailed internal information. The PFH liquid droplets with diameters of 7 μm were encapsulated in a PMSQ fibre of 10 μm diameter. This type of structure could potentially be used as a functional material, e.g. for textiles (Sun *et al.* 2003), as well as in drug delivery applications (Sill & Recum 2008).

3.4. Effect of applied voltage

The applied voltage between the needles and the ground electrode is the other key process control parameter (López-Herrera *et al.* 2003). In this study, the effects of applied voltage on hollow microsphere geometry and shell thickness at different voltages of 3.4, 3.8, 4.2 and 4.6 kV were investigated, while the polymer concentration was fixed at 36 wt%, and the flow rates in the inner and outer needles were kept at 150 and 300 μl min^{-1}, respectively. It was found (figure 7) that increasing the applied voltage resulted in a reduction in the mean microsphere diameter (*D*) from 810 nm at 3.4 kV to 370 nm at 4.6 kV. Thus, these results demonstrate that, by increasing the applied voltage, microspheres with diameter about four orders of magnitude smaller than the size of the outer needle can be produced. However, when the applied voltage is increased, the cone angle becomes larger and the acceleration distance to the exit of the outer needle becomes correspondingly shorter, so there will be a maximum voltage above which it is difficult to reach steady-state jetting. The mean shell thickness of hollow microspheres was 119 nm at 3.4 kV. By increasing the applied voltage to 3.8 kV, the mean thickness became smaller, reducing to 84 nm at 4.2 kV and 53 nm at 4.6 kV. The ratio α was almost constant at approximately 6.8.

3.5. Steady jetting region and D/t ratio

The driving liquid, which has a high viscosity and electrical conductivity, plays an essential role in the preparation of hollow microspheres and the spray phenomenon is mainly determined by the properties of the driving liquid (Loscertales *et al.* 2002). The relationship between applied voltage, flow rate and the onset of stable jetting at PMSQ concentrations of 18, 27 and 36 wt% was investigated (figure 8*a–c*). In each stable jet mode region, with all other parameters fixed, the applied voltage increased with increasing PMSQ flow rate. In addition, by increasing the PMSQ concentration from 18 to 36 wt%, the applied voltage needed to prepare hollow microspheres becomes higher and the magnitude between upper and lower voltages of cone-jet mode spraying decreases with the increase in the PMSQ concentration.

In this study, the ratio α provides important information for the preparation of capsules with predetermined mechanical properties and transportation behaviour of encapsulated bioactivity agents (Qiu *et al.* 2001; Dong *et al.* 2005; Rachik *et al.* 2006). In addition, the ratio of diameter to wall thickness produced by different processes is in the range of 5–30. It is clear that the production of a thinner shell will decrease the overall stiffness of the capsule wall (Rachik *et al.* 2006), and simultaneously increase the inner core volume while the diameter (*D*) is fixed. Over the entire parameter space, the largest value of α was achieved by a factor of approximately 10 at 18 wt% PMSQ while the smallest value of α (6.6) was obtained by increasing polymer concentration at 36 wt% PMSQ (figure 9). These hollow particles with a lower D/t ratio would be less prone to fragmentation, but have a smaller core volume.

3.6. Characterization of composition

FTIR spectra were obtained to confirm the composition of the hollow microspheres. Figure 10 shows infrared spectra of samples of native PMSQ powder and the microspheres over the wavenumber range from 400 to 4000 cm^{-1}. C–H vibrations of –CH, $-CH_2$ and $-CH_3$ groups showed absorption bands at around 2900 cm^{-1}. Less significant absorption was also observed at 2359 cm^{-1}, which may be attributed to residual carbon dioxide not purged from the FTIR spectrometer (C–O asymmetrical stretching vibration)

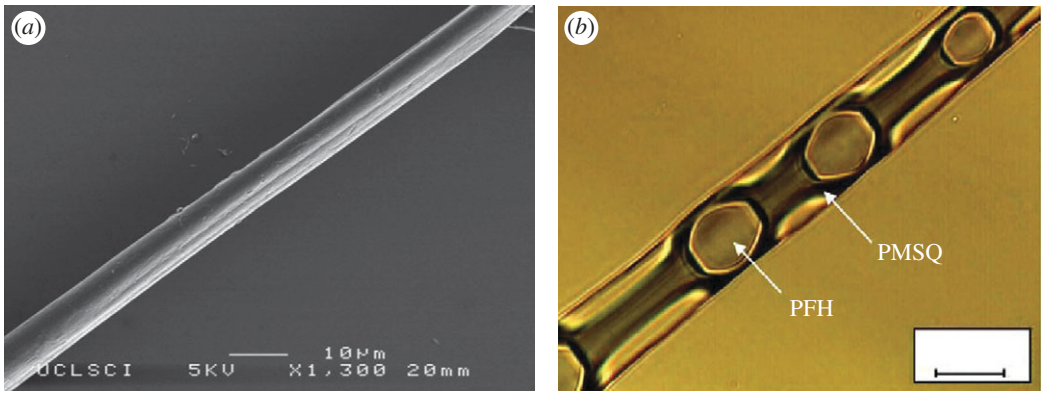

Figure 6. Effect of 63 wt% PMSQ concentration on the process product: (*a*) SEM image of PFH-loaded PMSQ fibre; (*b*) optical image of PFH-loaded PMSQ fibre. Scale bar, (*b*) 10 μm.

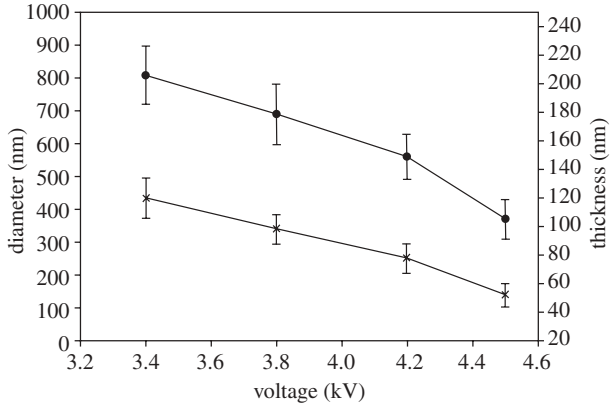

Figure 7. Size and shell thickness of microspheres versus applied voltage with inner flow rates of 150 μl min^{-1} and outer flow rate of 300 μl min^{-1} (error bars show standard deviation). Line with crosses, *D*; line with filled circles, *t*.

(Bogart *et al.* 1995). The methyl groups (CH_3) were also observed at absorption bands of 1410 and 1275 cm^{-1}, respectively. The typical absorption band of polysilsesquioxane at 1130 cm^{-1} was observed in both spectra (Ma *et al.* 2002). The two spectra are almost identical except for an additional absorption in the spectrum of 'dried hollow microsphere' at 1119 cm^{-1}. This is attributed to C_2F_6 (Eapen *et al.* 1994) and indicated that the PFH provides a volume for shell formation, after which it evaporated. Thus, the polymer is stable and not reactive with the PFH during processing, although there was some residual PFH in the hollow sphere.

3.7. Mechanism of hollow microsphere formation

PFH, which is a liquid at ambient temperature, is non-toxic and has been used in the preparation of multi-functional microspheres for medical and pharmaceutical applications (Giesecke & Hynynen 2003). The mechanism for the preparation of hollow microspheres takes advantage of its properties of immiscibility and volatility (Pisani *et al.* 2006). PFH and PMSQ were injected with appropriate flow rates under an applied voltage, in which the electrical forces acted on the

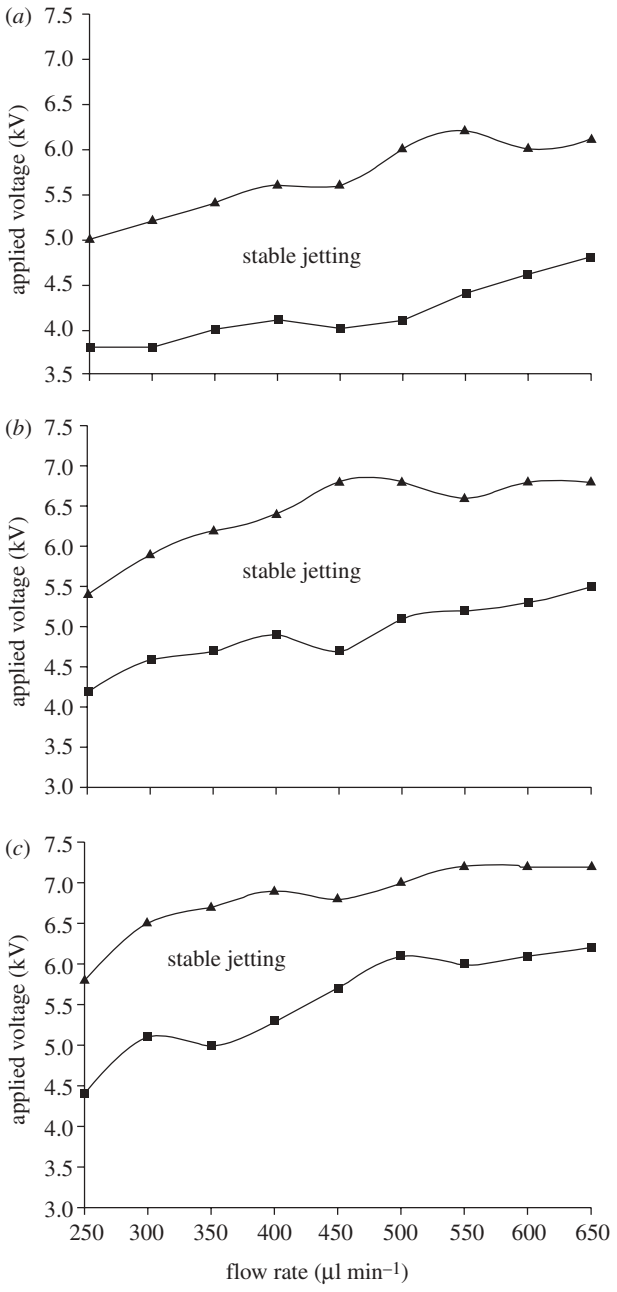

Figure 8. Mapping of applied voltage and flow rate of PMSQ at different PMSQ concentrations: (*a*) 18 wt%, (*b*) 27 wt% and (*c*) 36 wt%.

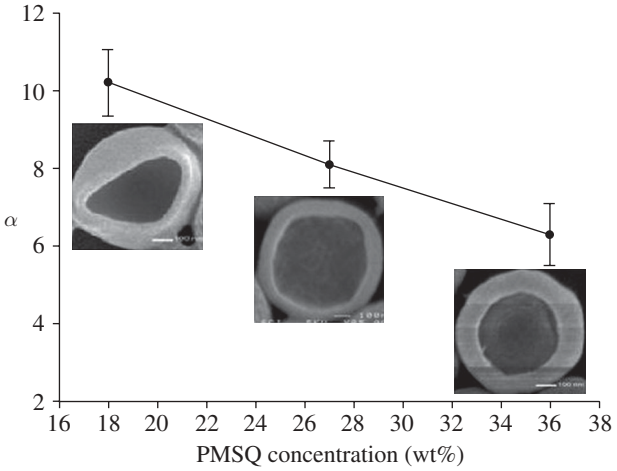

Figure 9. Variation of D/t ratio (α) with polymer concentration.

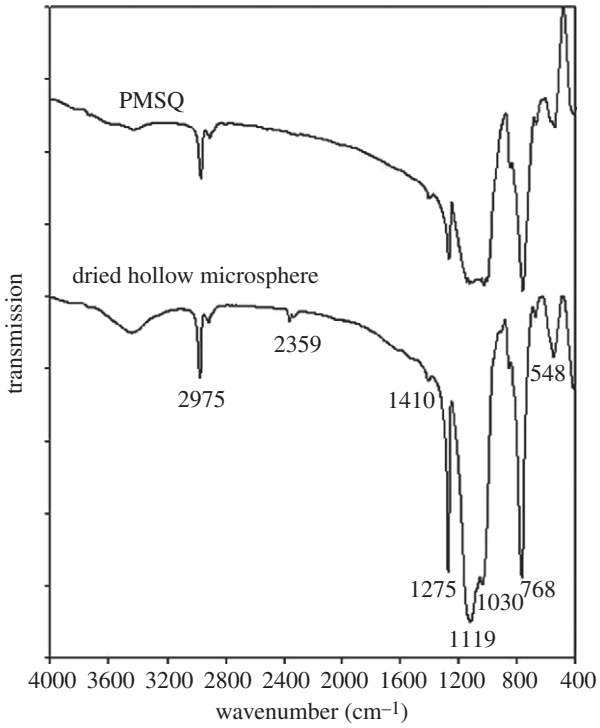

Figure 10. FTIR spectra of PMSQ and dried hollow microspheres.

driving liquid and led to the establishment of the cone. The PMSQ solution was accelerated by the electrical field, while the flow of PFH was dominated by viscous stresses. Hence, the electrical forces acting on the PMSQ film drive the inner viscous liquid so that both liquids flow steadily with the same velocity. Thus, concentric droplets can be obtained with PMSQ around the PFH; these are stable and retain their integrity owing to their immiscibility. The core material (PFH) can change phase from liquid to gas at ambient temperature owing to its low boiling point. The thin PMSQ layer contains nanopores and channels that can allow small molecules and ions to pass through the shell. After shell formation, the core liquid can thus be easily removed by gentle evaporation under ambient conditions owing to its volatility.

The use of PFH liquid droplets in this technique also paves the way for incorporating functional oils or oil-soluble compounds inside the particles. Apart from its non-toxicity, PFH is able to dissolve and deliver oxygen to several tissues (Riess 2001), and it can also be used as an external phase of emulsion to entrap lipophilic drugs into hydrophilic or lipophilic polymers (Mana *et al.* 2007). It is biocompatible against other solid templates and may allow facile and efficient introduction of functional liquid cores, drug and DNA molecules inside the capsule, which is particularly attractive in drug delivery and pharmaceutical applications. By partially evaporating the core, the microspheres would also be made amenable for stimulated release of the encapsulated material by thermal or ultrasonic excitation (Chang *et al.* 2009).

As mentioned earlier, the polymer shell used in this study (PMSQ) is both biocompatible and highly stable, and thus the microspheres produced were also resistant to degradation, showing no degradation over the course of the experimental work (several weeks) under ambient conditions. The two materials (PFH and PMSQ) were used in this work, however, simply to provide a model system to enable detailed characterization of the EHDA processing method. The relationship between the physical and electrical properties of the materials used and the characteristics of the capsules formed is demonstrated by the results shown above, and thus indicates that a wide range of materials could potentially be used for microsphere formation using this method. The selection would be determined mainly by the requirements of the particular application (e.g. the properties of the material to be encapsulated and the required degradation rate of the shell) rather than the constraints of the processing method.

The use of EHDA is by no means restricted to biomedical applications, but an important question in terms of the industrial application of EHDA is the yield of particles that may be obtained. For the single co-axial needle set used in this work, approximately 4.6×10^{10} particles min^{-1} were generated. Yield can of course be increased by the use of multiple needles as described by Bocanegra *et al.* (2005) and, as discussed in the introduction, EHDA is an efficient method for microcapsule preparation as it avoids the need for templating and template-removal steps required by other methods.

4. CONCLUSIONS

This study demonstrates that EHDA provides a means of preparing hollow polymeric microspheres with close control over their diameter and shell thickness. This method provides a simple mechanism to integrate the forming of a core-shell structure in one step and offers a simplified route avoiding complex procedures involving templating. It also eliminates the use of surfactants or additives in the forming process. In this study, controlling the surface morphology, shell

thickness and diameter of hollow microspheres was investigated in depth and results showed that the mean diameter of the hollow microsphere could be varied in the range from 310 to 1000 nm by adjusting the flow rate, polymer concentration or applied voltage. The shell thickness can be controlled by the polymer concentration. It is related to the outer diameter by a factor of 10 at polymer 18 wt%, a factor of 8.1 at 27 wt% and 6.6 at 36 wt%. However, at 63 wt%, hollow microspheres could not be obtained but PMSQ fibres with PFH liquid encapsulated can be generated.

The authors would like to thank the EPSRC and the Royal Academy of Engineering for supporting this work through Prof. Edirisinghe's Platform Grant (EP/E045839) and Dr Stride's Research Fellowship, respectively, and also UCL for supporting M.-W.C. through an Overseas Research Scholarship.

REFERENCES

Bai, M.-Y., Cheng, Y.-J., Wickline, S. A. & Xia, Y. 2009 Colloidal hollow spheres of conducting polymers with smooth surface and uniform, controllable sizes. *Small* **5**, 1747–1752. (doi:10.1002/smll.200900447)

Berkland, C., Pack, D. W. & Kim, K. K. K. 2004 Controlling surface nano-structure using flow-limited field-injection electrostatic spraying (FFESS) of poly(D,L-lactide-co-glycolide). *Biomaterials* **25**, 5649–5658. (doi:10.1016/j.biomaterials.2004.01.018)

Bocanegra, R., Galán, D., Márquez, M., Loscertales, I. & Barrero, A. 2005 Multiple electrosprays emitted from an array of holes. *J. Aerosol Sci.* **36**, 1387–1399. (doi:10.1016/j.jaerosci.2005.04.003)

Bogart, K. H. A., Dalleska, N. F., Bogart, G. R. & Fisher, E. R. 1995 Plasma enhanced chemical vapor deposition of SiO_2 using novel alkoxysilane precursors. *J. Vac. Sci. Technol. A Vac. Surf. Films* **13**, 476–480. (doi:10.1116/1.579382)

Caruso, F., Caruso, R. A. & Hwald, H. M. 1998 Nanoengineering of inorganic and hybrid hollow spheres by colloidal templating. *Science* **282**, 1111. (doi:10.1126/science.282.5391.1111)

Chang, M., Stride, E. & Edirisinghe, M. 2009 A novel process for drug encapsulation using a liquid to vapour phase change material. *Soft Matter* **5**, 5029–5036. (doi:10.1039/b913178g)

Chang, M., Stride, E. & Edirisinghe, M. 2010 A new method for the preparation of monoporous hollow microspheres. *Langmuir* **26**, 5115–5121. (doi:10.1021/la903592s)

Chen, D. & Jiang, M. 2005 Strategies for constructing polymeric micelles and hollow spheres in solution via specific intermolecular interactions. *Acc. Chem. Res.* **38**, 494–502. (doi:10.1021/ar040113d)

Daiguji, H., Makuta, T., Kinoshita, H., Oyabu, T. & Takemura, F. 2007 Fabrication of hollow melamine-formaldehyde microcapsules from microbubble templates. *J. Phys. Chem. B.* **111**, 8879–8884. (doi:10.1021/jp072131t)

de la Mora, J. F. D. L. & Loscertales, I. G. 1994 The current emitted by highly conducting Taylor cones. *J. Fluid Mech.* **260**, 155–184. (doi:10.1017/S0022112094003472)

Dong, W.-F., Ferri, J. K., Adalsteinsson, T., Schnhoff, M., Sukhorukov, G. B. & Mhwald, H. 2005 Influence of shell structure on stability, integrity, and mesh size of polyelectrolyte capsules: mechanism and strategy for improved preparation. *Chem. Mater.* **17**, 2603–2611. (doi:10.1021/cm050103m)

Dowding, P. J., Atkin, R., Vincent, B. & Bouillot, P. 2004 Oil core-polymer shell microcapsules prepared by internal phase separation from emulsion droplets. I. Characterization and release rates for microcapsules with polystyrene shells. *Langmuir* **20**, 11 374–11 379. (doi:10.1021/la048561h)

Eapen, K. C., John, P. J. & Liang, J. C. 1994 Degradation of a branched perfluoropolyalkyloether fluid with anhydrous aluminum-chloride. *Macromol. Chem. Phys.* **195**, 2887–2903. (doi:10.1002/macp.1994.021950818)

F2 Chemicals Ltd. 2010 Perfluorohexane. CAS number 355-42-0. See http://www.fluoros.co.uk/data/medical_applications/perfluorohexane.php.

Farook, U., Stride, E. & Edirisinghe, M. J. 2009 Preparation of suspensions of phospholipid-coated microbubbles by coaxial electrohydrodynamic atomization. *J. R. Soc. Interface* **6**, 271–277. (doi:10.1098/rsif.2008.0225)

Gao, F., Su, Z.-G., Wang, P. & Ma, H. 2009 Double emulsion templated microcapsules with single hollow cavities and thickness-controllable shells. *Langmuir* **25**, 3832–3838. (doi:10.1021/la804173b)

Giesecke, T. & Hynynen, K. 2003 Ultrasound-mediated cavitation thresholds of liquid perfluorocarbon droplets *in vitro*. *Ultrasound Med. Biol.* **29**, 1359–1365. (doi:10.1016/S0301-5629(03)00980-3)

Hartman, R. P. A., Brunner, D. J., Camelot, D. M. A., Marijnissen, J. C. M. & Scarlett, B. 1999 Electrohydrodynamic atomization in the cone-jet mode physical modeling of the liquid cone and jet. *J. Aerosol Sci.* **30**, 823–849. (doi:10.1016/S0021-8502(99)00033-6)

Hu, Y., Ding, Y., Ding, D., Sun, M., Zhang, L., Jiang, X. & Yang, C. 2007 Hollow chitosan/poly(acrylic acid) nanospheres as drug carriers. *Biomacromolecules* **8**, 1069–1107. (doi:10.1021/bm0608176)

Im, S. H., Jeong, U. & Xia, Y. 2005 Polymer hollow particles with controllable holes in their surfaces. *Nat. Mater.* **4**, 671–675. (doi:10.1038/nmat1448)

Kim, Y. B. & Yoon, S. 2004 A physical method of fabricating hollow polymer spheres directly from oil/water emulsions of solutions of polymers. *Macromol. Rapid Commun.* **25**, 1643–1649. (doi:10.1002/marc.200400203)

Lastowa, O. & Balachandran, W. 2006 Numerical simulation of electrohydrodynamic (EHD) atomization. *J. Electrostat.* **64**, 850–859. (doi:10.1016/j.elstat.2006.02.006)

Li, G., Yang, X. & Bai, F. 2007 A facile route to poly(divinylbenzene) hollow microspheres with pyridyl group on the interior surface. *Polymer* **48**, 3074–3081. (doi:10.1016/j.polymer.2007.03.066)

Li, X., Huang, J. & Edirisinghe, M. 2007 Development of nano-hydroxyapatite coating by electrohydrodynamic atomization spraying. *J. Mater. Sci. Mater. Med.* **19**, 1545–1551. (doi:10.1007/s10856-007-3303-3)

Liu, G., Zhang, H., Yang, X. & Wang, Y. 2007 Facile synthesis of silica/polymer hybrid microspheres and hollow polymer microspheres. *Polymer* **48**, 5896–5904. (doi:10.1016/j.polymer.2007.07.068)

Liu, Q., Huang, C., Luo, S., Liu, Z. & Liu, B. 2007 Production of micron-sized hollow microspheres by suspension polymerization of St-DEGDA (diethylene glycol diacrylate) with petroleum ether (90–120°C). *Polymer* **48**, 1567–1572. (doi:10.1016/j.polymer.2007.01.034)

López-Herrera, J. M., Barrero, A., López, A., Loscertales, I. G. & Márqueze, M. 2003 Coaxial jets generated from electrified Taylor cones. Scaling laws. *J. Aerosol Sci.* **34**, 535–552. (doi:10.1016/S0021-8502(03)00021-1)

Loscertales, I. G., Barrero, A., Guerrero, I., Cortijo, R., Marquez, M. & Gañán-Calvo, A. M. 2002 Micro/nano encapsulation via electrified coaxial liquid jets. *Science* **295**, 1695–1698. (doi:10.1126/science.1067595)

Lou, X. W., Archer, L. A. & Yang, Z. 2008 Hollow micro-/nanostructures: synthesis and applications. *Adv. Mater.* **20**, 3987–4019. (doi:10.1002/adma.200800854)

Lynch, D. E., Nawaz, Y. & Bostrom, T. 2005 Preparation of sub-micrometer silica shells using poly(1-methylpyrrol-2-ylsquaraine). *Langmuir* **21**, 6572–6575. (doi:10.1021/la0506933)

Ma, J., Feng, Q. Y., Shi, L. H. & Xu, J. 2002 Preliminary study on pyrolysis of polymethylsilsesquioxane by FT-IR and XPS. *Chin. Chem. Lett.* **13**, 75–78.

Mana, Z., Pellequer, Y. & Lamprecht, A. 2007 Oil-in-oil microencapsulation technique with an external perfluorohexane phase. *Int. J. Pharm.* **338**, 231–237. (doi:10.1016/j.ijpharm.2007.02.010)

Munir, M. M., Suryamas, A. B., Iskandar, F. & Okuyama, K. 2009 Scaling law on particle-to-fibre formation during electrospinning. *Polymer* **50**, 4935–4943. (doi:10.1016/j.polymer.2009.08.011)

Nangrejo, M., Ahmad, Z., Stride, E. & Edirisinghe, M. 2008 Preparation of polymeric and ceramic porous capsules by a novel electrohydrodynamic process. *Pharm. Dev. Technol.* **13**, 425–432. (doi:10.1080/10837450802247929)

Okubo, M., Konishi, Y. & Minami, H. 2000 Production of hollow polymer particles by suspension polymerizations for divinylbenzene/toluene droplets dissolving various polymers. *Colloid Polym. Sci.* **278**, 659–664. (doi:10.1007/s003960000308)

Pareta, R. & Edirisinghe, M. J. 2006 A novel method for the preparation of biodegradable microspheres for protein drug delivery. *J. R. Soc. Interface* **3**, 573–582. (doi:10.1098/rsif.2006.0120)

Pisani, E., Tsapis, N., Paris, J., Nicolas, V., Cattel, L. & Fattal, E. 2006 Polymeric nano/microcapsules of liquid perfluorocarbons for ultrasonic imaging: physical characterization. *Langmuir* **22**, 4397–4402. (doi:10.1021/la0601455)

Qiu, X., Leporatti, S., Donath, E. & Mhwald, H. 2001 Studies on the drug release properties of polysaccharide multilayers encapsulated ibuprofen microparticles. *Langmuir* **17**, 5375–5380. (doi:10.1021/la010201w)

Rachik, M., Barthes-Biesel, D., Carin, M. & Edwards-Levy, F. 2006 Identification of the elastic properties of an artificial capsule membrane with the compression test: effect of thickness. *J. Colloid Interface Sci.* **301**, 217–226. (doi:10.1016/j.jcis.2006.04.062)

Riess, J. G. 2001 Oxygen carriers ('blood substitutes'): raison d'etre, chemistry, and some physiology—blut ist ein ganz besondrer saft. *Am. Chem. Rev.* **101**, 2797–2920. (doi:10.1021/cr970143c)

Shchukin, D. G., Sukhorukov, G. B. & Hwald, H. M. 2003 Biomimetic fabrication of nanoengineered hydroxyapatite/polyelectrolyte composite shell. *Chem. Mater.* **15**, 3947–3950. (doi:10.1021/cm0341585)

Shiomi, T., Tsunoda, T., Kawai, A., Matsuura, S.-I., Mizukami, F. & Sakaguch, K. 2009 Synthesis of a cagelike hollow aluminosilicate with vermiculate micro-through-holes and its application to ship-in-bottle encapsulation of protein. *Small* **5**, 67–71. (doi:10.1002/smll.200800834)

Sill, T. J. & Recum, H. A. V. 2008 Electrospinning: applications in drug delivery and tissue engineering. *Biomaterials* **29**, 1989–2006. (doi:10.1016/j.biomaterials.2008.01.011)

Song, L., Ge, X., Wang, M. & Li, Z. Z. S. 2006 Anionic/nonionic mixed surfactants templates preparation of hollow polymer spheres via emulsion polymerization. *J. Polym. Sci. Part A Polym. Chem.* **44**, 2533–2541. (doi:10.1002/pola.21322)

Sun, Z., Zussman, E., Yarin, A. L., Wendorff, J. H. & Greiner, A. 2003 Compound core-shell polymer nanofibres by co-electrospinning. *Adv. Mater.* **15**, 1929. (doi:10.1002/adma.200305136)

Utada, A. S., Lorenceau, E., Link, D. R., Kaplan, P. D., Stone, H. A. & Weitz, D. A. 2005 Monodisperse double emulsions generated from a microcapillary device. *Science* **308**, 537–541. (doi:10.1126/science.1109164)

Valo, H., Peltonen, L., Vehvilainen, S., Karjalainen, M., Kostiainen, R., Laaksonen, T. & Hirvonen, J. 2009 Electrospray encapsulation of hydrophilic and hydrophobic drugs in poly(L-lactic acid) nanoparticles. *Small* **5**, 1791–1798. (doi:10.1002/smll.200801907)

Wang, D. & Caruso, F. 2002 Polyelectrolyte-coated colloid spheres as templates for sol–gel reactions. *Chem. Mater.* **14**, 1909–1913. (doi:10.1021/cm0211251)

Wang, Q., Liu, Y. & Yan, H. 2007 Mechanism of a self-templating synthesis of monodispersed hollow silica nanospheres with tunable size and shell thickness. *Chem. Commun.* **23**, 2339–2341. (doi:10.1039/b701572k)

Wu, M., Neill, S. A. O., Brousseau, L. C., Mcconnell, W. P., Shultz, D. A., Linderman, R. J. & Feldheim, D. L. 2000 Synthesis of nanometer-sized hollow polymer capsules from alkanethiol-coated gold particles. *Chem. Commun.* **9**, 775–776. (doi:10.1039/b001019g)

Xiao, D. S., Yuan, Y. C., Rong, M. Z. & Zhang, M. Q. 2009 Hollow polymeric microcapsules: preparation, characterization and application in holding boron trifluoride diethyl etherate. *Polymer* **50**, 560–568. (doi:10.1016/j.polymer.2008.11.022)

Xie, J., Marijnissen, J. C. M. & Wang, H. 2006 Microparticles developed by electrohydrodynamic atomization for the local delivery of anticancer drug to treat C6 glioma *in vitro*. *Biomaterials* **27**, 3321–3332. (doi:10.1016/j.biomaterials.2006.01.034)

Xu, X. & Asher, S. A. 2004 Synthesis and utilization of monodisperse hollow polymeric particles in photonic crystals. *J. Am. Chem. Soc.* **126**, 7940–7945. (doi:10.1021/ja049453k)

Yan, E., Ding, Y., Chen, C., Li, R., Hu, Y. & Jiang, X. 2009 Polymer/silica hybrid hollow nanospheres with pH-sensitive drug release in physiological and intracellular environments. *Chem. Commun.* **19**, 2718–2720. (doi:10.1039/b900751b)

Zhang, L., Peng, H., Sui, J., Soeller, C., Kilmartin, P. A. & Travas-Sejdic, J. 2009 Self-assembly of poly(o-methoxyaniline) hollow microspheres. *J. Phys. Chem. C* **113**, 9128–9134. (doi:10.1021/jp900267t)

Zimmermann, C., Feldmann, C., Wanner, M. & Gerthsen, D. 2009 Solid-to-hollow single-particle manipulation of a self-assembled luminescent NaYF4 : Yb,Er nanocrystal monolayer by electron-beam lithography. *Small* **5**, 2057–2060. (doi:10.1002/smll.200900404)

Zoldesi, C. I. & Imhof, A. 2005 Synthesis of monodisperse colloidal spheres, capsules, and microballoons by emulsion templating. *Adv. Mater.* **17**, 924–928. (doi:10.1002/adma.200401183)